Pramana – J. Phys. (2021) 95:208
https://doi.org/10.1007/s12043-021-02235-5

Enhanced Raman gain coefficients (under steady-state and transient regimes) of semiconductor magnetoplasmas

JAIVIR SINGH[1], SUNITA DAHIYA[1] and MANJEET SINGH[2,*]

[1]Department of Physics, Baba Mastnath University, Asthal Bohar, Rohtak 124 021, India
[2]Department of Physics, Government College, Matanhail, Jhajjar 124 106, India
*Corresponding author. E-mail: msgur_18@yahoo.com

MS received 7 June 2021; accepted 29 July 2021

Abstract. Assuming the origination of stimulated Raman scattering (SRS) in Raman susceptibility, we obtain expressions for Raman gain coefficients (under steady-state and transient regimes) of semiconductor magnetoplasmas under various geometrical configurations. The threshold value of excitation intensity and most favourable value of pulse duration (above which transient Raman gain vanishes) are estimated. For numerical calculations, we consider n-InSb crystal at 77 K temperature as a Raman-active medium exposed to a frequency doubled pulsed CO_2 laser. The variation of Raman gain coefficients on doping concentration, magnetostatic field and its inclination, scattering angle and pump pulse duration have been explored in detail with an aim to determine suitable values of these controllable parameters to enhance Raman gain coefficients at lower threshold intensities and to establish the suitability of semiconductor magnetoplasmas as hosts for compression of scattered pulses and fabrication of efficient Raman amplifiers and oscillators based on Raman nonlinearities.

Keywords. Laser–plasma interaction; Raman gain; threshold intensity; semiconductor plasmas.

PACS Nos 52.38.-r; 72.30.+q; 42.65.Dr; 78.55.Cr

1. Introduction

Nonlinear optics is a broad field of research and technology that encompasses laser–matter interaction. It gives increasing attention due to its interesting applications such as ultrashort pulsed lasers, ultrafast switches, laser amplifiers and oscillators, optical signal processing, optical sensors, optical computers and many others [1–5]. Nonlinear optical effects (NLOEs) can be usually classified into two broad areas: steady-state (SS) NLOEs and transient (TR) NLOEs [6]. SS-NLOEs occur as an outcome of cw laser–matter interaction. Moreover, SS-NLOEs (TR-NLOEs) occur with pulsed laser–matter interaction such that the laser pulse duration is sufficiently greater (smaller) than the recombination time of the excited carriers of the medium. The fast development of femtosecond lasers has made it possible to observe TR-NLOEs in a variety of materials [7].

Out of various SS-NLOEs, stimulated scatterings of laser radiation have been an active field of research; on the one hand, they provide essential information of the laser–matter interaction, and on the other hand they lead to numerous applications in nonlinear optics [8,9]. When a coherent (pump) wave travels through a nonlinear medium, under certain conditions, it excites the natural vibrational modes (i.e. electron–plasma and ion waves) of the medium. The high frequency excited mode scatters the pump wave at Stokes and anti-Stokes shifted frequencies giving rise to the phenomenon of stimulated Raman scattering (SRS). SRS is an important NLOE and it has widespread applications in nonlinear optics. It has been used to broaden the tuning range of coherent radiation sources over the broad infrared spectrum regime [10,11]. SRS anti-Stokes radiation has been used to generate extreme ultraviolet radiation for applications in high-resolution absorption spectroscopy [12]. Various forms of SRS spectroscopy include a wide range of applications [13,14]: scientific research in cell biology, detection of explosives, identification of polymorphism of substances, non-destructive identification of substances etc.

SRS has been extensively studied in solids, liquids, gases and plasmas and hence extensive literature has been accumulated on various aspects of this phenomenon. The new development of techniques for the fabrication of nonlinear materials hassignificantly con-

Published online: 30 November 2021

tributed to this progress. Among various nonlinear materials, semiconductor plasmas possess large optical nonlinearities (which can be further significantly enhanced by their magnetisation) and satisfy at the same time all the technological necessities including high damage threshold, fast response time and wide transparency range for potential applications in optoelectronic devices and hence prove to be advantageous hosts for studying the important phenomenon of SRS [15].

Up to now, SRS has been studied in semiconductor magnetoplasmas by classical, semiclassical and quantum mechanical approach by several research groups [16–21]. In all these studies:

(i) the phenomenon has been studied in the steady-state regime,
(ii) the propagation of scattered radiation has been considered in the backward direction only,
(iii) the semiconductor plasma has been magnetised by applying an external magnetostatic field either parallel to the pump wave propagation (Faraday geometry) or perpendicular to the pump wave propagation (Voigt geometry),
(iv) the origin of the SRS in polar semiconductor magnetoplasmas has been considered in finite differential polarisability only.

However, the study of SRS under transient regime provides a better understanding of the laser–plasma interaction and idea of compression of laser pulses. Also, in SRS the scattered radiation propagates in backward direction and also scatters in all possible directions, i.e. forward to backward scattering. Moreover, the semiconductor plasma can be magnetised by applying an external magnetostatic field in any direction (from Faraday to Voigt geometry) to the pump wave propagation. Furthermore, in III–V semiconductor plasmas, being weakly polar, the coupling between the pump field and the excited vibrational modes not only depends on finiteness of differential polarisability (DP) but also depend upon Szigeti effective charge (SEC) which must be included in infrared laser–semiconductor plasma interaction [22]. Therefore, the inclusion of SEC in analytical investigations of SRS in semiconductor plasmas appears to be important from both the fundamental as well as application viewpoints. These warrant that the phenomenon of SRS should be treated under SS and TR regimes under various geometrical configurations of external magnetostatic field with the incorporation of SEC in the analysis.

TR-SRS has been widely used for pulse compression (ns to sub-ns) in liquids and gaseous media [23]. SRS has been successfully used for cw [24], ns [25] and ps [26] pulsed lasers. The SS and TR optical nonlinearities of a nonlinear medium are, in general, related to other [27]. Using this methodology and treating the semiconductor magnetoplasma as a Raman active medium, we develop a theoretical model to study the SS- and TR-SRS under various geometrical configurations of external magnetostatic field. Third-order (Raman) susceptibility and consequent SS and TR Raman gain coefficients are obtained using the coupled-mode theory of plasmas. Numerical calculations are made for n-InSb–CO_2 laser system. Efforts are directed to enhance the SS and TR Raman gain coefficients at lower threshold intensities by adjusting the material parameters and geometry of the applied magnetostatic field, and to explore the feasibility of semiconductor magnetoplasmas for the fabrication of efficient Raman amplifiers and oscillators.

2. Theoretical formulations

In this section, expressions for effective Raman susceptibility and hence SS and TR Raman gain coefficients, threshold pump intensity for exciting TR-SRS and the most favourable value of pulse duration (above which TR Raman gain vanishes) are obtained.

2.1 *Induced current density*

Let us consider the well-known hydrodynamic model of semiconductor plasmas. This model remains valid only in the limit [28]: $k_{op}l \ll 1$; k_{op} and l being the wave number of the excited molecular vibrational mode and mean free path of the carriers (here electrons), respectively. In a semiconductor plasma, SRS arises due to nonlinear interactions among three coherent fields, which in the present case are:

(i) an intense pump field $E_0(x,t) = E_0 \exp[i(k_0 x - \omega_0 t)]$,
(ii) an induced molecular vibrational mode $u(x,t) = u_0 \exp[i(k_{op}x - \omega_{op}t)]$, and
(iii) a scattered Stokes component of the pump field $E_s(x,t) = E_s \exp[i(k_s x - \omega_s t)]$.

The momentum and energy conservation relations to be satisfied among these waves are: $\hbar\vec{k}_0 = \hbar\vec{k}_{op} + \hbar\vec{k}_s$ and $\hbar\omega_0 = \hbar\omega_{op} + \hbar\omega_s$, respectively. The relation between the magnitude of the three wave vectors may be represented as: $k_{op} = (k_0^2 + k_s^2 - 2k_0k_s\cos\phi)^{1/2}$, where ϕ is the scattering angle between $\vec{k}_s$ and $\vec{k}_0$. Let us consider the semiconductor plasma immersed in an external magnetostatic field $\vec{B}_0$ in a direction making an arbitrary angle θ with the x-axis (i.e. direction of propagation of the pump wave) in the x–z plane.

In semiconductor plasmas, the origin of SRS lies in nonlinear coupling between electron plasma wave and molecular vibrational mode caused by the pump wave. The molecular vibrational mode generates fluctuations (at molecular vibrational frequency ω_{op}) in electron concentration in the Raman medium which, in turn, couples nonlinearly with the pump wave under the influence of external magnetostatic field and regenerates the electron plasma wave at modified frequency. Thus, at the expense of the pump wave, the electron plasma wave and molecular vibrational mode derive one another in semiconductor magnetoplasmas.

The semiconductor magnetoplasma consists of N independent harmonic oscillators per unit volume. Each oscillator stands for a vibrational mode of one molecule and is characterised by its molecular weight M, and its normal vibrational coordinates $u(x,t)$. The equation describing the motion of a single oscillator, including the contributions of SEC (q_s) and DP ($\alpha_u = (\partial\alpha/\partial u)_0$) is given by [19]

$$\frac{\partial^2 u}{\partial t^2} + \Gamma\frac{\partial u}{\partial t} + \omega_{opo}^2 u = \frac{1}{M}\left[q_s E + \frac{1}{2}\varepsilon\alpha_u \bar{E}^2(x,t)\right], \tag{1}$$

where Γ is the phenomenological damping constant (responsible for the linewidth of spontaneous Raman scattering) and ω_{opo} is the undamped molecular vibrational frequency. These two parameters are related to each other via the relation: $\gamma \approx 10^{-2}\omega_{opo}$ [29]. The quantity inside the square bracket on the RHS of eq. (1) represents the effective driving force per unit volume; the first and second terms stand for the contributions arising due to q_s and α_u of the Raman medium. $\varepsilon = \varepsilon_0\varepsilon_\infty$ where ε_0 and ε_∞ are the absolute permittivity and high-frequency dielectric constant of the Raman medium.

The other equations taken in the coupled mode approach are:

$$\frac{\partial \vec{v}_0}{\partial t} + \nu\vec{v}_0 = -\frac{e}{m}[\vec{E}_0 + (\vec{v}_0 \times \vec{B}_0)] = -\frac{e}{m}(\vec{E}_e) \tag{2}$$

$$\frac{\partial \vec{v}_1}{\partial t} + \nu\vec{v}_1 + \left(\vec{v}_0\frac{\partial}{\partial x}\right)\vec{v}_1 = -\frac{e}{m}[\vec{E}_1 + (\vec{v}_1 \times \vec{B}_0)] \tag{3}$$

$$\frac{\partial n_1}{\partial t} + n_0\frac{\partial v_1}{\partial x} + n_1\frac{\partial v_0}{\partial x} + v_0\frac{\partial n_1}{\partial x} = 0 \tag{4}$$

$$\vec{P}_{mv} = \varepsilon N\alpha_u u^* \vec{E}_e \tag{5}$$

$$\frac{\partial E_{1x}}{\partial x} + \frac{1}{\varepsilon}\frac{\partial}{\partial x}(|\vec{P}_{mv}|) = -\frac{n_1 e}{\varepsilon}. \tag{6}$$

Equations (2) and (3) represent the equilibrium and perturbed electron momentum transfer equations. Equation (4) is the well-known electron continuity equation. Here, n_0, $\vec{v}_0$ and $\vec{v}_1, n_1$ are the equilibrium and perturbed electron concentrations and electron fluid velocities, respectively. ν is the electron collision frequency. Equation (5) gives the molecular vibrational polarisation $\vec{P}_{mv}$. The space charge electric field E_{1x} can be deduced from eq. (6).

The molecular vibrational mode (at frequency ω_{op}) modulates the relative permittivity of the Raman medium and causes power transfer among those radiation fields which differ in frequency by multiples of ω_{op} (i.e., $\omega_0 \pm p\omega_{op}$, where $p = 1, 2, 3,...$). The modes at the difference $(\omega_0 - p\omega_{op})$ and sum $(\omega_0 + p\omega_{op})$ frequencies are known as Stokes and anti-Stokes modes, respectively. Here, the anti-Stokes modes and higher-order Stokes modes (with $p \geq 2$) have been neglected [19]. The first-order Stokes mode (with $p = 1$) which acts as a primary source of Raman amplification is considered.

Using eqs (1) – (6) and the phase-matching conditions, the perturbed electron concentrations (n_{1op} and n_{1s}) of the Raman medium due to molecular vibrations and first-order Stokes mode can be deduced by following the procedure adopted in ref. [19] as:

$$n_{1op} = \frac{[2iMk_{op}(\omega_t^2 - \omega_{op}^2 + i\Gamma\omega_{op}) - \varepsilon N]A}{e\alpha_u E_0^*}u^* \tag{7}$$

and

$$n_{1s} = \frac{ie(k_0 - k_{op})E_0}{m(\omega_{rs}^2 - i\nu\omega_s)}n_{1op}^*. \tag{8}$$

In eq. (7),

$$A = \frac{2q_s\alpha_u}{\varepsilon} - \alpha_u^2|E_0|^2.$$

In eq. (8)

$$\omega_{rs}^2 = \bar{\omega}_r^2 - \omega_s^2,$$

where

$$\bar{\omega}_r^2 = \omega_r^2\left(\frac{\nu^2 + \omega_{cx,z}^2}{\nu^2 + \omega_c^2}\right)$$

is the coupled electron plasmon–cyclotron frequency, in which

$$\omega_r^2 = \frac{\omega_p^2\omega_l^2}{\omega_t^2}$$

and

$$\omega_{cx,z} = \frac{e}{m}B_{sx,z}$$

are the components of electron–cyclotron frequency ω_c along the x- and z-axes,

$$\omega_p = \left(\frac{n_0 e^2}{m\varepsilon_0\varepsilon_L}\right)^{1/2}$$ (electron plasma frequency) and

$$\frac{\omega_l}{\omega_t} = \left(\frac{\varepsilon_L}{\varepsilon_\infty}\right)^{1/2}.$$

$$\omega_l = \frac{k_B \theta_D}{\hbar}$$

is the longitudinal molecular vibrational frequency, in which k_B is the Boltzmann constant, θ_D is the Debye temperature of the semiconductor plasma and $\hbar = \frac{h}{2\pi}$; h being the Plancks constant and ε_L is the dielectric constant of the Raman medium.

From eq. (2), the components of the electron fluid velocity ($v_{0x,y}$) under the influence of the pump and external magnetostatic fields are obtained as

$$v_{0x} = \frac{\bar{E}}{\nu - i\omega_0}$$

and

$$v_{0y} = \frac{(e/m)[\omega_c + (\nu - i\omega_0)]E_0}{[\omega_c^2 + (\nu - i\omega_0)^2]}. \tag{9}$$

The (resonant) Stokes component of the electron current density ($J_{cd}(\omega_s)$); neglecting the transition dipole moment is obtained as

$$J_{cd}(\omega_s) = n_{1s}^* e v_{0x} = \frac{\varepsilon k_{op}(k_0 - k_{op})\left|\bar{E}_0\right|^2 E_1}{(\omega_{rs}^2 + i\nu\omega_s)(\nu - i\omega_s)} \times \left[1 - \frac{\varepsilon N A}{2M(\omega_{rop}^2 + i\Gamma\omega_{op})}\right], \tag{10}$$

where $\omega_{rop}^2 = \bar{\omega}_r^2 - \omega_{op}^2$.

2.2 *Effective Raman susceptibility*

The nonlinear induced polarisation ($P_{cd}(\omega_s)$), which may be defined as the time integral of the induced current density, is given by

$$P_{cd}(\omega_s) = \int J_{cd}(\omega_s)\,\mathrm{d}t = \frac{\varepsilon_\infty e^2 k_{op}(k_0 - k_{op})\left|\bar{E}_0\right|^2 E_1}{m^2\omega_0\omega_s(\omega_{rs}^2 + i\nu\omega_s)} \times \left[1 - \frac{\varepsilon N A}{2M(\omega_{rop}^2 + i\Gamma\omega_{op})}\right]. \tag{11}$$

Defining the induced polarisation (at ω_s) as

$$P_{cd}(\omega_s) = \varepsilon_0(\chi_R^{(3)})_{cd}\left|\bar{E}_0\right|^2 E_1,$$

the Raman susceptibility $(\chi_R^{(3)})_{cd}$ is given by

$$(\chi_R^{(3)})_{cd} = \frac{\varepsilon_\infty e^2 k_{op}(k_0 - k_{op})}{\varepsilon_0 m^2\omega_0\omega_s(\omega_{rs}^2 + i\nu\omega_s)} \times \left[1 - \frac{N}{M(\omega_{rop}^2 + i\Gamma\omega_{op})} \times \left(q_s\alpha_u - \frac{\varepsilon_L\alpha_u^2}{\eta c} I_0\right)\right], \tag{12}$$

where

$$I_0 = \frac{1}{2}\eta c\varepsilon_0 |E_0|^2$$

represents the pump intensity, in which η stands for the background refractive index of the Raman medium and c is the speed of light in the Raman medium which is given by $c_0/(\varepsilon_L)^{1/2}$.

In addition to $P_{cd}(\omega_s)$, the Raman medium also possesses a polarisation $P_{mv}(\omega_s)$, the origin of which lies in the pump–molecular vibrational mode interaction. Using eqs (1) and (5), one obtains

$$P_{mv}(\omega_s) = \frac{\varepsilon^2\omega_0^2 N\alpha_u}{2M(\omega_c^2 + i\Gamma\omega_{op})}|E_0|^2 E_1. \tag{13}$$

Consequently, the corresponding Raman susceptibility $(\chi_R^{(3)})_{mv}$ is given by

$$(\chi_R^{(3)})_{mv} = \frac{\varepsilon^2\omega_0^2 N\alpha_u}{2\varepsilon_0 M(\omega_c^2 + i\Gamma\omega_{op})}. \tag{14}$$

The effective Raman susceptibility in a Raman medium is given by

$$\begin{aligned}(\chi_R^{(3)})_{\text{eff}} &= (\chi_R^{(3)})_{mv} + (\chi_R^{(3)})_{cd} \\ &= \frac{\varepsilon^2\omega_0^2 N\alpha_u}{2\varepsilon_0 M(\omega_c^2 + i\Gamma\omega_{op})} \\ &\quad + \frac{\varepsilon_\infty e^2 k_{op}(k_0 - k_{op})}{\varepsilon_0 m^2\omega_0\omega_s(\omega_{rs}^2 + i\nu\omega_s)} \\ &\quad \times \left[1 - \frac{N}{M(\omega_{rop}^2 + i\Gamma\omega_{op})} \times \left(q_s\alpha_u - \frac{\varepsilon_L\alpha_u^2}{\eta c} I_0\right)\right].\end{aligned} \tag{15}$$

We observed that $(\chi_R^{(3)})_{\text{eff}}$ is a complex quantity and it can be written as

$$(\chi_R^{(3)})_{\text{eff}} = [(\chi_R^{(3)})_{\text{eff}}]_r + i[(\chi_R^{(2)})_{\text{eff}}]_i,$$

where $[(\chi_R^{(3)})_{\text{eff}}]_r$ and $[(\chi_R^{(3)})_{\text{eff}}]_i$ represent the real and imaginary parts of $(\chi_R^{(3)})_{\text{eff}}$, respectively. Rationalising eq. (15), we get

$$\begin{aligned}[(\chi_R^{(3)})_{\text{eff}}]_r &= \frac{\varepsilon^2\omega_0^2 N\alpha_u\omega_c^2}{2\varepsilon_0 M(\omega_c^4 + \Gamma^2\omega_{op}^2)} \\ &\quad + \frac{\varepsilon_\infty e^2 k_{op}(k_0 - k_{op})\omega_{rs}^2}{\varepsilon_0 m^2\omega_0\omega_s(\omega_{rs}^4 + \nu^2\omega_s^2)} \\ &\quad \times \left[1 - \frac{N\omega_{rop}^2}{M(\omega_{rop}^4 + \Gamma^2\omega_{op}^2)}\right.\end{aligned}$$

$$\times \left(q_s \alpha_u - \frac{\varepsilon_L \alpha_u^2}{\eta c} I_0 \right) \Bigg] \tag{15a}$$

$$[(\chi_{\mathrm{R}}^{(3)})_{\mathrm{eff}}]_i = -\frac{\varepsilon^2 \omega_0^2 N \alpha_u \Gamma \omega_{op}}{2\varepsilon_0 M(\omega_c^4 + \Gamma^2 \omega_{op}^2)} - \frac{\varepsilon_\infty e^2 k_{op}(k_0 - k_{op}) \nu \omega_s}{\varepsilon_0 m^2 \omega_0 \omega_s (\omega_{rs}^4 + \nu^2 \omega_s^2)} \times \left[1 + \frac{N \Gamma \omega_{op}}{M(\omega_{rop}^4 + \Gamma^2 \omega_{op}^2)} \times \left(q_s \alpha_u - \frac{\varepsilon_L \alpha_u^2}{\eta c} I_0 \right) \right]. \tag{15b}$$

Equations (15a) and (15b) show that both $[(\chi_{\mathrm{R}}^{(3)})_{\mathrm{eff}}]_r$ as well as $[(\chi_{\mathrm{R}}^{(3)})_{\mathrm{eff}}]_i$ are influenced by q_s, α_u, n_0 (via ω_p), B_0 (via ω_c) and I_0.

2.3 *SS and TR Raman gain coefficients*

At pump intensities well above the threshold value, the SS Raman gain coefficient $(g_{\mathrm{R}})_{ss}$ is obtained via the well-known relation:

$$(g_{\mathrm{R}})_{ss} = -\frac{k_s}{4\eta^3 \varepsilon_0 c}[(\chi_{\mathrm{R}}^{(3)})_{\mathrm{eff}}]_i I_0 = \frac{\varepsilon^2 k_s \omega_0^2 N \alpha_u \Gamma \omega_{op} I_0}{8\varepsilon_0^2 \eta^3 c M(\omega_c^4 + \Gamma^2 \omega_{op}^2)} + \frac{\varepsilon_\infty e^2 k_s k_{op}(k_0 - k_{op}) \nu \omega_s I_0}{4\varepsilon_0^2 \eta^3 c m^2 \omega_0 \omega_s (\omega_{rs}^4 + \nu^2 \omega_s^2)} \times \left[1 + \frac{N \Gamma \omega_{op}}{M(\omega_{rop}^4 + \Gamma^2 \omega_{op}^2)} \times \left(q_s \alpha_u - \frac{\varepsilon_L \alpha_u^2}{\eta c} I_0 \right) \right]. \tag{16}$$

From eq. (16), we find that $(g_{\mathrm{R}})_{ss}$ consists of two terms: the first term occurs due to the finiteness of α_u only while the second term occurs due to the finiteness of both q_s and α_u. It is interesting to note that for parameters of n-InSb–CO_2 laser system given in §3, at pump intensities $I_0 < I_c (= 2.5 \times 10^{13}\ \mathrm{W\ m^{-2}})$, $q_s \alpha_u > (\varepsilon_L \alpha_u^2 / \eta c) I_0$ and both q_s as well as α_u contribute to $(g_{\mathrm{R}})_{ss}$ while at $I_0 > I_c (= 2.5 \times 10^{13}\ \mathrm{W\ m^{-2}})$, $q_s \alpha_u < (\varepsilon_L \alpha_u^2 / \eta c) I_0$ and the contributions of q_s diminish and hence $(g_{\mathrm{R}})_{ss}$ becomes dependent on α_u only. Thus, at moderate pump intensities ($I_0 > I_c$), the Szigeti effective charge significantly contributes to Raman gain.

Further, eq. (16) reveals that $(g_{\mathrm{R}})_{ss}$ increases linearly with I_0. Practically, however, an arbitrary increase in I_0 may damage the sample. According to Mayer *et al* [30], when a semiconductor plasma is irradiated by an intense long pulsed laser, the frequent outcome is the heat generation. Kruer *et al* [31] found that a pump intensity of ~$10^{11}\ \mathrm{W\ m^{-2}}$ of Q-switched 170 ns pulse frequency doubled 10.6 μm CO_2 laser damages InSb at 300 K. The damage threshold intensity of the semiconductor plasma can be increased by the free carrier nonlinear absorption or by reducing the duration of the pump pulse [32]. Due to the threshold nature of SRS, it is observed at high pump intensities and hence the pulsed lasers are generally employed in SRS experiments. For SRS and resulting Raman amplification to occur, an intense pump wave with ns or sub-ns pulse duration is desired. These pulse durations are of the order of molecular vibrational mode lifetime ($\tau_p \sim \Gamma_{\mathrm{R}}^{-1}$), and under such conditions, instead of SS gain coefficient $(g_{\mathrm{R}})_{ss}$, $(g_{\mathrm{R}})_{ss}\Gamma_{\mathrm{R}}$ is a more important gain parameter. This parameter suggests an idea of Stokes pulse compression [33]. It is thus clear from the above discussion that SRS must be treated under coherent transient excitation regime. The TR Raman gain coefficient $(g_{\mathrm{R}})_{tr}$ of a nonlinear medium may be obtained as [27]

$$(g_{\mathrm{R}})_{tr} = (2(g_{\mathrm{R}})_{ss} L \Gamma_{\mathrm{R}} \tau_p)^{1/2} - \Gamma_{\mathrm{R}} \tau_p, \tag{17}$$

where $\Gamma_{\mathrm{R}} \tau_p < (g_{\mathrm{R}})_{ss} L$, in which Γ_{R} is the molecular vibrational mode lifetime, τ_p is the pump pulse duration and L is the interaction path length. For backward SRS ($\phi = 180°$) at very short pump pulse duration ($\tau_p \leq 10^{-10}$ s), one may replace L by $c\tau_p/2$.

2.4 *Threshold pump intensity and most favourable pulse duration for TR Raman gain*

For backward TR-SRS, the threshold pump intensity $(I_{0,th,tr})$ is obtained, by making $(g_{\mathrm{R}})_{tr} = 0$ in eq. (17), as

$$I_{0,th,tr} = \frac{\Gamma_{\mathrm{R}} \tau_p}{2c(G_{\mathrm{R}})_{ss}}, \tag{18}$$

where

$$(G_{\mathrm{R}})_{ss} = \frac{(g_{\mathrm{R}})_{ss}}{I_0}.$$

Using $\Gamma_{\mathrm{R}} = 3.7 \times 10^{11}\ \mathrm{s^{-1}}$ and $(g_{\mathrm{R}})_{ss} = 50\ \mathrm{m^{-1}}$ at $I_0 = 2.85 \times 10^9\ \mathrm{W\ m^{-2}}$ for n-InSb–CO_2 laser system and eq. (18), one finds $I_{0,th,tr} = 1.5 \times 10^{11}\ \mathrm{W\ m^{-2}}$. However, for $\tau_p \geq 10^{-9}$ s, the Raman cell length is taken equal to L, and under such a condition one obtains

$$(g_{\mathrm{R}})_{tr} = (\Gamma_{\mathrm{R}} \tau_p)^{1/2}[(2(g_{\mathrm{R}})_{ss} L)^{1/2} - (\Gamma_{\mathrm{R}} \tau_p)^{1/2}]. \tag{19}$$

This expression suggests an idea to determine the most favourable value of pulse duration ($(\tau_p)_{\mathrm{opt}}$), above which the transient Raman gain vanishes. This can be obtained by making $(g_{\mathrm{R}})_{tr} = 0$ in eq. (19), as

$$(\tau_p)_{\mathrm{opt}} \approx \frac{(g_{\mathrm{R}})_{ss}}{\Gamma_{\mathrm{R}}}. \tag{20}$$

A calculation for n-InSb–CO_2 laser system using the values given earlier and $L = 10^{-4}$ m gives $(\tau_p)_{\text{opt}} = 5.6 \times 10^{-20} I_0$ s. This value of $(\tau_p)_{\text{opt}}$ not only explains the washing out of TR Raman gain at large pulse duration but also suggests that the most favourable value of pulse duration can be increased by increasing the intensity of the pump wave.

3. Results and discussion

In order to study the dependence of SS and TR Raman gain coefficients on external magnetostatic field and its inclination, and scattering angle, let us consider n-InSb sample as a Raman medium illuminated by 10.6 μm CO_2 at 77 K. For n-InSb crystal, $m = 0.014 m_0$, where m_0 is the rest mass of electrons. The other material parameters are taken as follows [19]: $\varepsilon_L = 17.8$, $\varepsilon_\infty = 15.68, \eta = 4.2, \nu = 3.5 \times 10^{11}\ \text{s}^{-1}, \rho = 5.8 \times 10^3$ kg m^{-3}, $\Gamma_R = 3.7 \times 10^{11}\ \text{s}^{-1}$, $N = 1.48 \times 10^{28}\ \text{m}^{-3}$, $M = 2.7 \times 10^{-29}$ kg, $\alpha_u = 1.68 \times 10^{-16}$ SI units, $q_s = 1.2 \times 10^{-20}$ C, $\omega_0 = 1.78 \times 10^{14}\ \text{s}^{-1}$, $\omega_{op} = 3.64 \times 10^{13}\ \text{s}^{-1}$.

The present analytical investigation explains the dependence of SS and TR Raman gain coefficients ($(g_R)_{ss}$ and $(g_R)_{tr}$) on controllable parameters such as doping concentration (n_0), external magnetostatic field (B_0), magnetostatic field inclination (θ), scattering angle (ϕ), pump pulse duration (τ_p) etc. Equations (16), (19) and (20) are used to study $(g_R)_{ss}$ and $(g_R)_{tr}$ by varying the controllable parameters: n_0, B_0, θ, ϕ and τ_p. Efforts are made for:

(i) determining appropriate values of these controllable parameters to enhance SS and TR Raman gain coefficients at lower threshold intensities, and
(ii) exploring the possibility of Raman nonlinearities -dependent efficient semiconductor devices.

Figure 1 shows the variation of $(g_R)_{ss}$ and $(g_R)_{tr}$ with B_0 for two different values of n_0. It can be observed that both $(g_R)_{ss}$ and $(g_R)_{tr}$ show similar nature of curves throughout the plotted regime of B_0. The nature of the curves can be explained as follows: By keeping n_0 fixed and varying B_0, we observed that the gain coefficients are comparatively smaller and remain independent of the magnetostatic field in the regimes $0 < B_0 < 10$ T and $0 < B_0 < 2$ T for $n_0 = 2 \times 10^{23}\ \text{m}^{-3}$ and $3 \times 10^{23}\ \text{m}^{-3}$, respectively. By further increasing B_0 beyond this value, the gain coefficients start increasing, achieving their peaks at $B_0 = 11$ T and 3 T for $n_0 = 2 \times 10^{23}\ \text{m}^{-3}$ and $3 \times 10^{23}\ \text{m}^{-3}$, respectively. By further increasing B_0 slightly beyond these values, the gain coefficients decrease sharply and attain their previously lower value at $B_0 = 12$ T and 4 T for $n_0 = 2 \times 10^{23}\ \text{m}^{-3}$ and $3 \times 10^{23}\ \text{m}^{-3}$, respectively and remain constant for $B_0 = 13$ T. This distinct behaviour of gain coefficients occurs due to the resonance condition, $\bar{\omega}_r^2 \sim \omega_s^2$. Further $\bar{\omega}_r^2$ being the function of ω_p and ω_c can be varied by changing either/both B_0 and n_0. It is advantageous to shift ω_s in desired spectral regime in proportion to: (i) n_0 (or ω_p) for fixed B_0 (or ω_c), (ii) B_0 (or ω_c) for fixed n_0 (or ω_p) and (iii) combination of both n_0 and B_0. Continuously increasing n_0 (via ω_p and hence $\bar{\omega}_r^2$) and decreasing B_0 (via ω_c and hence $\bar{\omega}_r^2$) in the same proportion maintains $\bar{\omega}_r^2 \sim \omega_s^2$ and keeps ω_s fixed. Further, by continuously increasing n_0 and decreasing B_0 without maintaining their proportion maintains $\bar{\omega}_r^2 \sim \omega_s^2$ but shifts ω_s at other value. For the n-InSb–CO_2 laser system, by continuously increasing n_0 from $2 \times 10^{23}\ \text{m}^{-3}$ to $3 \times 10^{23}\ \text{m}^{-3}$ and decreasing B_0 from 11 T to 3 T maintains $\omega_s^2 \sim \bar{\omega}_r^2$ and keeps ω_s fixed at $1.77 \times 10^{14}\ \text{s}^{-1}$. Ultimately, at $n_0 = 3.3 \times 10^{23}\ \text{m}^{-3}$, the resonance occurs around $B_0 = 0$ T for a fixed value of ω_s. For $n_0 > 3.3 \times 10^{23}\ \text{m}^{-3}$, the resonance condition shifts the value of ω_s.

When $B_0 = 13$ T, the gain coefficients corresponding to two different values of doping concentration as reported above become equal and exhibit common behaviour independent of doping concentration for $B_0 \geq 13$ T. The gain coefficients show a common peak at $B_0 = 14.2$ T. This peak occurs due to the resonance condition, $\omega_c^2 \sim \omega_0^2$. Around resonance, electrons drift velocity increases and exceeds the molecular vibrational mode velocity and as a result the pump to molecular vibrational mode energy transfer increases, and consequently molecular vibrational mode amplifies. Eventually, the amplified molecular vibrational mode feeds more energy from the pump to the scattered Raman Stokes mode, thereby enhancing the SS and TR Raman gain coefficients.

An important aspect of this analysis is an enhancement of SS and TR Raman gain coefficients around resonance conditions by varying simultaneously/independently the doping concentration and magnetostatic field in semiconductor plasmas. The results obtained in figure 1 permits the tuning of the scattered Raman Stokes mode and opens up an opportunity of fabrication of frequency converters based on Raman amplification as well as tunable Raman oscillators.

Figure 2 shows the variation of $(g_R)_{ss}$ and $(g_R)_{tr}$ with θ for $\phi = 0°$ (forward scattering) and $\phi = 180°$ (backward scattering). One can observe that in both the cases, the Raman gain coefficients are comparatively smaller in the case of Faraday geometry (i.e. $\theta = 0°$). The gain coefficients continuously increase with θ in the regime $\theta < 90°$, achieving maximum at $\theta = 90°$ and decrease

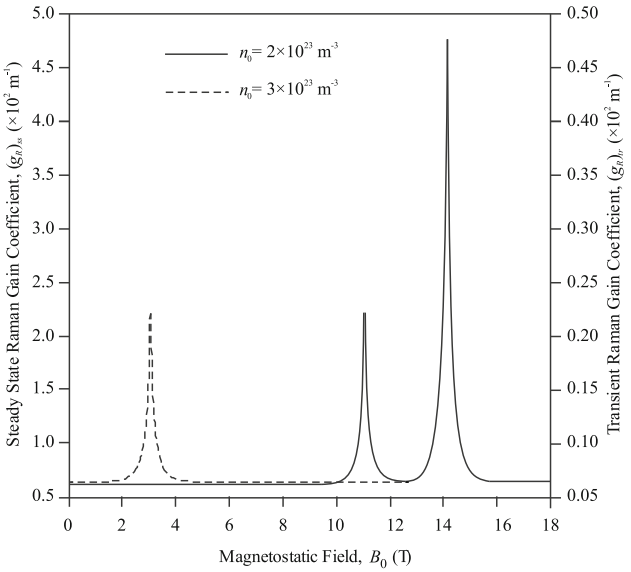

Figure 1. Variation of $(g_R)_{ss}$ and $(g_R)_{tr}$ with B_0 for $n_0 = 2 \times 10^{23}$ m^{-3} and 3×10^{23} m^{-3}. Here $\theta = 60°$, $\phi = 45°$, $\tau_p = 5 \times 10^{-10}$ s.

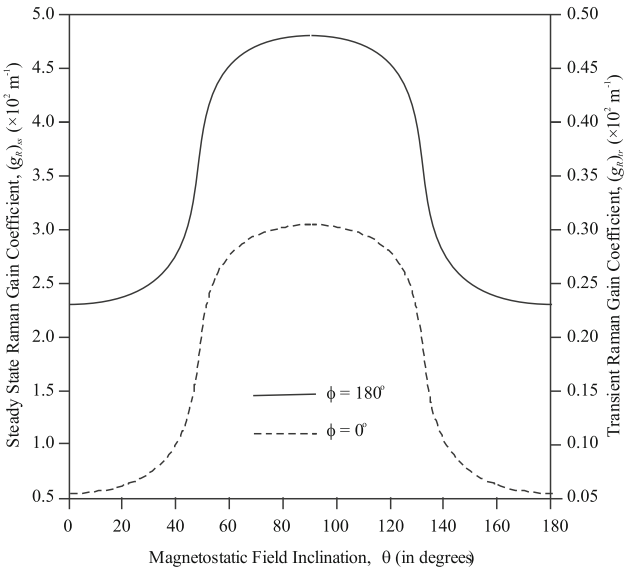

Figure 2. Variation of $(g_R)_{ss}$ and $(g_R)_{tr}$ with θ for $\phi = 0°$ and 180°. Here $n_0 = 2 \times 10^{23}$m^{-3}, $\phi = 45°$, $\tau_p = 5 \times 10^{-10}$ s.

with θ in the regime $\theta > 90°$. The rate of rise (fall) of gain coefficients is higher in the regimes $20° < \theta < 70°$ ($110° < \theta < 160°$). The curves are symmetrical about $\theta = 90°$. The curves infer that the contribution of magnetic Lorentz force, which plays a significant role in modifying the electron's drift velocity, and consequently the energy transfer from the pump to scattered Stokes wave and subsequently enhancing the SS and TR Raman gain coefficients is maximum in the case of Voigt geometry (i.e. $\theta = 90°$). Moreover, the gain coefficients are

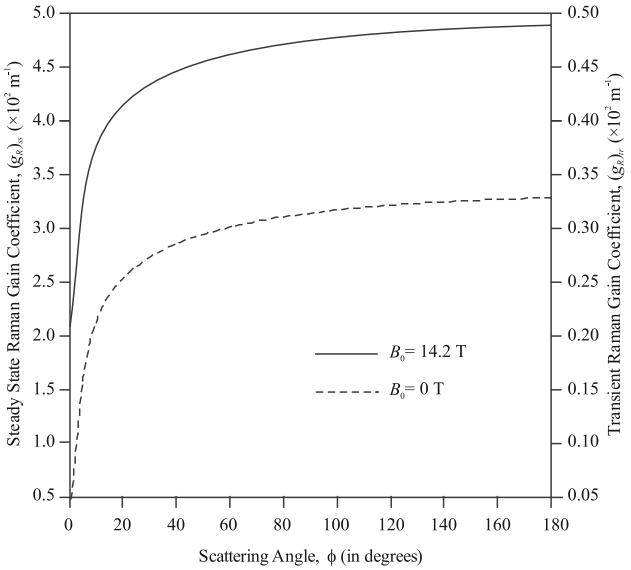

Figure 3. Variation of $(g_R)_{ss}$ and $(g_R)_{tr}$ with ϕ for $B_0 = 0$ T and 14.2 T. Here $n_0 = 2 \times 10^{23}$ m^{-3}, $\theta = 60°$, $\tau_p = 5 \times 10^{-10}$ s.

six times higher under Voigt geometry than under Faraday geometry. In addition, the gain coefficients are four times higher for backward scattering than for forward scattering throughout the plotted range of magnetic field inclination.

Figure 3 shows the variation of $(g_R)_{ss}$ and $(g_R)_{tr}$ with ϕ in the absence ($B_0 = 0$ T) and presence ($B_0 = 14.2$ T) of the magnetostatic field. It is clear that in both the cases, the Raman gain coefficients are larger in the forward scattering direction (i.e., $\phi = 0°$). However, the scattered Raman Stokes mode grows exponentially between $0° < \phi < 40°$ and thereafter the growth rate decreases, finally saturates around $\phi = 180°$. The comparison between the forward and backward SRS reveals that the Raman gain coefficients in the case of backward scattering are almost double compared to the case of forward scattering. In addition, the gain coefficients are four times higher in the presence of external magnetostatic field than in the absence external magnetostatic field throughout the plotted range of scattering angle.

Figure 4 shows the variation of threshold intensity ($(I_{0,th})_{tr}$) for the onset of TR-SRS with magnetostatic field (B_0) for two different pump pulse durations. It can be seen that in both the cases, $(I_{0,th})_{tr}$ decreases gradually with B_0 for $B_0 < 11$ T. The nature of curves indicates that the Lorentz contribution is very small when $\omega_c < \omega_0$. However, when ω_c approaches ω_0, the Lorentz contribution becomes effective to minimise the value of $(I_{0,th})_{tr}$. When $\omega_c > \omega_0$ (i.e. $B_0 > 14.2$ T), $(I_{0,th})_{tr}$ increases sharply and remains constant even at larger B_0. A comparison between the two

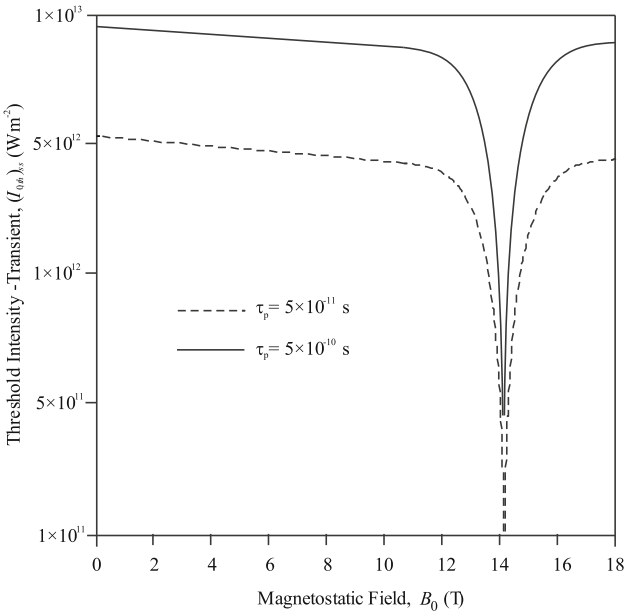

Figure 4. Variation of $(I_{0,th})_{tr}$ with B_0 for $\tau_p = 5 \times 10^{-10}$ s and 5×10^{-11} s. Here $n_0 = 4.5 \times 10^{23}$ m^{-3}, $\theta = 60°$, $\phi = 45°$.

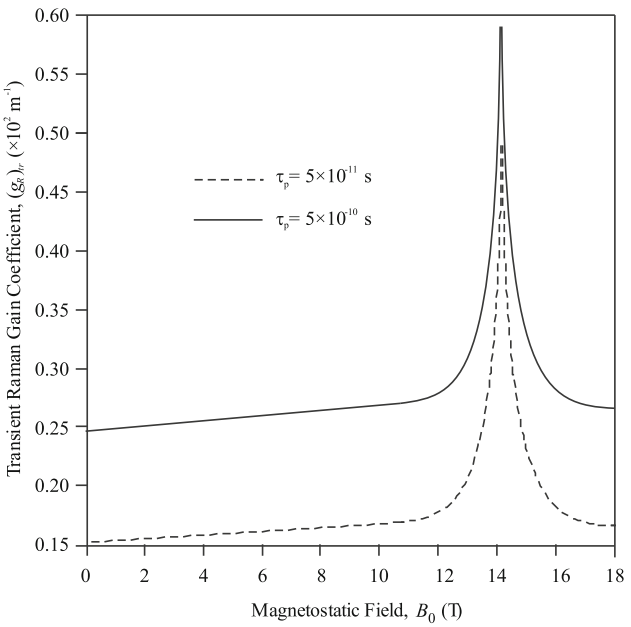

Figure 5. Variation of $(g_R)_{tr}$ with B_0 for $\tau_p = 5 \times 10^{-10}$ s and 5×10^{-11} s. Here $n_0 = 4.5 \times 10^{23}$ m^{-3}, $\theta = 60°$, $\phi = 45°$, $(I_{0,th})_{tr} = 5 \times 10^{12}$ W m^{-2}.

curves reveals that $(I_{0,th})_{tr}$ is lower at smaller values of τ_p.

Figure 5 shows the variation of $(g_R)_{tr}$ with B_0 for two different pump pulse durations. One can observe that in both the cases, $(g_R)_{tr}$ increases gradually with B_0 for $B_0 < 11$ T. This feature indicates that the Lorentz contribution is very small when $\omega_c < \omega_0$. However, when

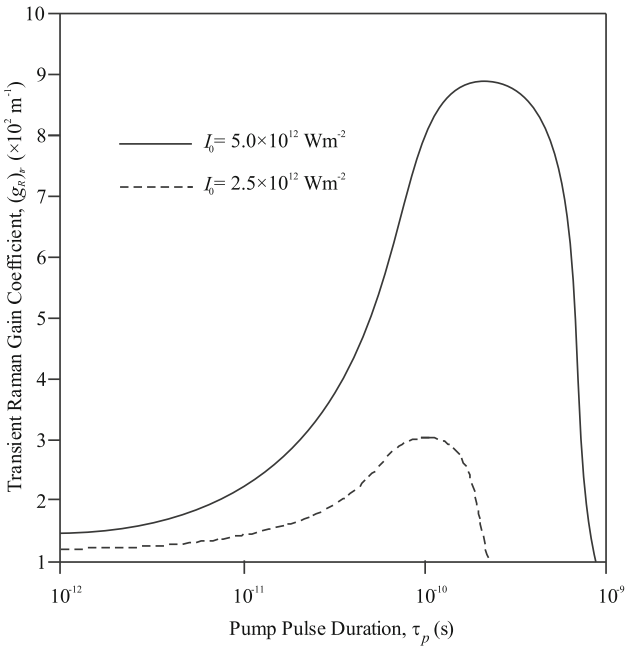

Figure 6. Variation of $(g_R)_{tr}$ with τ_p for $I_0 = 2.5 \times 10^{12}$ W m^{-2} and 5.0×10^{12} W m^{-2}. Here $n_0 = 4.5 \times 10^{23}$ m^{-3}, $B_0 = 14.2$ T, $\theta = 60°$, $\phi = 45°$.

ω_c approaches ω_0, the Lorentz contribution becomes effective to enhance the value of $(g_R)_{tr}$. When $\omega_c > \omega_0$ (i.e. $B_0 > 14.2$ T), $(g_R)_{tr}$ decreases sharply and remains constant even at larger B_0. A comparison between the two curves reveals that $(g_R)_{tr}$ is larger at larger values of τ_p.

Figure 6 shows the variation of $(g_R)_{tr}$ with τ_p (in the range 10^{-12} s $\leq \tau_p \leq 10^{-9}$ s) for two different pump intensities. We observed that for fixed I_0, $(g_R)_{tr}$ increases with τ_p and at a certain value of τ_p, $(g_R)_{tr}$ arrives at a certain maximum value which remains constant over a narrow range of τ_p. Such regimes may be termed as quasi-SS regimes. By increasing τ_p beyond the quasi-SS regime, $(g_R)_{tr}$ falls off rapidly. The rise in I_0 enhances $(g_R)_{tr}$ considerably over the entire plotted range of τ_p but shifts the quasi-SS regime towards higher values of τ_p. This behaviour suggests the idea of compression of scattered Raman Stokes pulses.

4. Conclusions

This paper presents a theoretical study of SS and TR Raman gain coefficients in semiconductor magnetoplasmas. Important conclusions drawn from the study are

1. The analysis offers two achievable resonance conditions ($\omega_s^2 \sim \bar{\omega}_r^2$ and $\omega_0^2 \sim \omega_c^2$) in which

significant enhancement of SS and TR Raman gain coefficients can be obtained.

2. The SS and TR Raman gain coefficients are six times higher under Voigt geometry than under Faraday geometry, four times higher for backward scattering than for forward scattering, and four times higher in the presence of external magnetostatic field than in its absence.
3. The rise in pump intensity shifts the Raman gain quasi-SS regime towards higher values of pump pulse duration. For example, in n-InSb semiconductor plasma, the quasisaturation regime which occurs around $\tau_p = 10^{-10}$ s at $I_0 = 2.5 \times 10^{12}$ W m^{-2} shifts to $\tau_p = 3.5 \times 10^{-10}$ s at $I_0 = 5 \times 10^{12}$ W m^{-2}.
4. The suitability of semiconductor magnetoplasmas as hosts for compression of scattered pulses and fabrication of efficient Raman amplifiers and oscillators based on Raman nonlinearities is established.

Acknowledgements

The authors are very thankful to Sh. Vijay Singh Dahiya, Director General, Higher Education Department, Panchkula (Haryana) for his kind cooperation and Mrs Neelam Sheoran, Principal, Government College Matanhail, Jhajjar (Haryana) for valuable ideas to carry out this work.

References

[1] E Garmire, *Opt. Exp*. **21**, 30532 (2013)
[2] T Kobayashi, *Photonics* **5**, 19 (2018)
[3] Y Ji, H Wang, J Cui, M Yu, Z Yang and L Bai, *Photon. Netw. Commun*. **38**, 14 (2019)
[4] M Ono, M Hata, M Tsunekawa, K Nozaki, H Sumikura, H Chiba and M Notomi, *Nature Photon.* **14**, 37 (2020)
[5] T Hao, Y Liu, J Tang, Q Cen, W Li, N Zhu, Y Dai and J Capmany, *Adv. Photon.* **2**, 044001 (2020)
[6] R W Boyd, *Nonlinear optics*, 3rd Edn (Academic Press, New York, 2008)
[7] D Tan, K N Sharafudeen, Y Yue and J Qiu, *Prog. Mater. Sci*. **76**, 154 (2016)
[8] O Frazao, C Correia, M R M Racco Giraldi, M B Marques, H M Salgado, M A G Martinez, J C W A Costa, A P Barbero and J M Baptista, *The Open Opt. J.* **3**, 1 (2009)
[9] E Garmire, *New J. Phys*. **19**, 011003 (2017)
[10] D C Hanna, M A Yuratich and D Cottor, Nonlinear optics of free atoms and molecules, *Springer Series in optical science* (Springer-Verlag, Berlin, 1979) Vol. 17, Ch. 7.
[11] T R Loree, R C Sze, D L Barker and P B Scott, *IEEE J. Quantum Electron*. **15**, 337 (1979)
[12] J E Rothenberg, J F Young and S E Harris, *Opt. Lett*. **6**, 363 (1981)
[13] R S Das and T K Agrawal, *Vib. Spectrosc*. **57**, 163 (2011)
[14] Y Li, B Shen, S Li, Y Zhao, J Qu and L Liu, *Adv. Biol.* **5**, 2000184 (2021)
[15] J Singh, S Dahiya and M Singh, *Mater. Today: Proc*. **46**, 5844 (2021)
[16] S Guha and N Apte, *Pramana – J. Phys.* **16**, 99 (1981)
[17] P Sen and P K Sen, *Phys. Rev. B* **31**, 1034 (1985)
[18] A Neogi and S Ghosh, *Phys. Rev. B* **44**, 13074 (1991)
[19] M Singh, P Aghamkar, N Kishore, P K Sen and M R Perrone, *Phys. Rev. B* **76**, 012302 (2007)
[20] P Kumar and V K Tripathi, *J. Appl. Phys*. **107**, 103314 (2010)
[21] V P Singh and M Singh, *Opt. Quant. Electron*. **48**, 479 (2016)
[22] K S Srivastava, R Srivastava, A Sinha, A Tandon and A N Nigam, *Phys. Rev. B* **38**, 1357 (1988)
[23] Y Vida, T Nagahara, S Zaitsu, M Mateus and T Imasaka, *Opt. Exp*. **14**, 3083 (2006)
[24] C H Bryanat and M Golombok, *Opt. Lett*. **16**, 602 (1991)
[25] Y Ping, R K Kirkwood, T L Wang, D S Clark, S C Wilks, N Meezan, R L Berger, J Wurtele, N J Fisch, V M Malkin, E J Valeo, S F Martins and C Joshi, *Phys. Plasmas* **16**, 123113 (2009)
[26] I Tsymbalov, D Gorlova and A Savel'ev, *Phys. Rev. E* **102**, 063206 (2020)
[27] R L Carman, F Shimizu, C S Wang and N Bloembergen, *Phys. Rev. A* **2**, 60 (1970)
[28] S G Chefranov and A S Chefranov, Hydrodynamic methods and exact solutions in applications to the electromagnetic field theory in medium, in: *Nonlinear optics – Novel results in field theory in medium* edited by B Lembrikov (Intechopen, UK, 2020)
[29] S S Mitra and N E Massa, *Handbook on semiconductors* edited by T S Moss (North-Holland, Amsterdam, 1982)
[30] J M Mayer, F J Bartoli and M R Kruer, *Phys. Rev. B* **21**, 1559 (1980)
[31] M Kruer, L Esterowitz, F Bartoli and R Allea, The role of carrier diffusion in laser damage of semiconductor materials, in: *Laser induced damage in optical materials* edited by A J Glass and A H Guenther, NBS Special Publication No. 509 (Washington,1977) pp. 473–480
[32] T F Boggess, A Smirl, S Moss, I Boyd and E V Stryland, *IEEE J. Quantum Electron*. **21**, 488 (1985)
[33] D Phol and W Kaiser, *Phys. Rev. B* **1**, 31 (1970)